Interdomain Interactions between the Hydrophilic Domains of the Mannitol Transporter of *Escherichia coli* in the Unphosphorylated and Phosphorylated States†

Wim Meijberg, Gea K. Schuurman-Wolters, and George T. Robillard*

Department of Biochemistry and Groningen Biomolecular Sciences and Biotechnology Institute (GBB), University of Groningen, Nijenborgh 4, 9747 AG Groningen, The Netherlands

Received October 27, 1995; Revised Manuscript Received December 18, 1995⊗

ABSTRACT: Interdomain interactions in the mannitol-specific enzyme II of the phosphoenolpyruvate-dependent phosphotransferase system of *Escherichia coli* play a key role in the mechanism of mannitol transport across the membrane [Boer et al. (1995) *Biochemistry 34*, 3239−3247; Lolkema et al. (1991) *Biochemistry 30*, 6716−6721]. In this study, we focus on the interactions between the hydrophilic A and B domains and try to determine those as a function of the phosphorylation state of the enzyme. To this end, unfolding studies on the subcloned domains IIA^{mtl} and IIB^{mtl}, as well as on the binary combination $IIBA^{mtl}$, were performed, both in the unphosphorylated and in the phosphorylated states, using GuHCl and heat as the denaturant. It is shown that IIA^{mtl} and IIB^{mtl}, as well as P-IIA^{mtl} and P-IIB^{mtl}, unfold according to a two-state mechanism but that $IIBA^{mtl}$ and P_2-$IIBA^{mtl}$ do not exhibit such behavior. Two transitions are observed instead, indicating a lack of strong positive cooperative interactions. DSC studies of the unphosphorylated proteins showed a destabilization of the B domain in $IIBA^{mtl}$ with respect to the free IIB^{mtl} as indicated by a lowering of the melting temperature and a lower enthalpy of unfolding. Furthermore, it is shown that phosphorylation has a destabilizing effect on both IIA^{mtl} and $IIBA^{mtl}$ but not on IIB^{mtl}. Possible explanations for this behavior and the biological relevance of the destabilizing forces in $IIBA^{mtl}$ are discussed.

Enzyme $II^{mannitol}$ is the mannitol-specific transmembrane protein of the phosphoenolpyruvate-dependent phosphotransferase system of *Escherichia coli* (PTS)[1] [for reviews, see Lolkema and Robillard (1992) and Postma et al. (1993)]. The protein catalyzes the concomitant phosphorylation and transport of mannitol across the membrane at the expense of phosphoenolpyruvate. It consists of two C-terminal cytoplasmic domains, A and B,[2] and one transmembrane domain, C, where the mannitol binding site is located. The cytoplasmic domains contain one phosphorylation site each, His554 on the A domain (van Dijk et al., 1992a) and Cys384 on the B domain (Pas & Robillard, 1988; Pas et al., 1988, 1991). The A domain is phosphorylated by P-HPr and transfers the phosphoryl group to the B domain from which it is transferred to the carbohydrate during transport.

Many EII's have been identified in *E. coli* and other microorganisms over the years and a number of common features have become apparent. In all systems, A, B, and C domains functionally related to those in EII^{mtl} could be identified, some covalently linked to each other, some free. It is not known whether there is a structural or mechanistic reason for this. Information that could contribute to answering this question can be obtained from a quantitative assessment of the free energy of interaction between the domains. For example, studies of the kinetics of mannitol transport in site-directed mutants of EII^{mtl} and wild-type EII^{mtl} have shown that the B and C domains influence each other's conformation as a function of the phosphorylation state of the B domain (Boer et al., 1995; Lolkema et al., 1991). It is believed that a concomitant change in the interaction energy plays a key role in the mechanism of transport.

This study will focus on the interactions between the hydrophilic A and B domains of EII^{mtl}. Both domains as well as the binary combination, $IIBA^{mtl}$, were previously subcloned and shown to be enzymatically active (Van Weeghel et al., 1991a,b; Robillard et al., 1993). $IIBA^{mtl}$ is a monomer of 31.7 kDa, containing five tyrosines, four in the A domain and one in the B domain, and no tryptophans. The molecular masses of IIA^{mtl} and IIB^{mtl} are 16.4 and 15.3 kDa, respectively. The active site cysteine of the B domain is sensitive to oxidation, resulting in irreversible inactivation of the protein, a process which can be prevented by adding a small amount of a reducing agent, like mercaptoethanol or glutathione.

In recent years, a large number of unfolding studies have been performed on proteins containing more than one

† This research was supported by the Netherlands Foundation for the Life Sciences (SLW) with financial aid from the Netherlands Organization for Scientific Research (NWO).

* To whom correspondence should be addressed. Telephone: 050-3634321. Telefax: 050-3634165. E-mail: ROBILLARD@CHEM.RUG.NL.

⊗ Abstract published in *Advance ACS Abstracts*, February 1, 1996.

[1] Abbreviations: EI, enzyme I; EII, enzyme II; HPr, histidine-containing protein; PEP, phosphoenolpyruvate; PTS, phosphoenolpyruvate-dependent phosphotransferase system; GuHCl, guanidine hydrochloride; Hepes, *N*-2-(hydroxyethyl)piperazine-*N′*-2-ethanesulfonic acid; DSC, differential scanning calorimetry; LEM, linear extrapolation method; cel, cellobiose; glc, glucose; man, mannose; mtl, mannitol; ΔH^{cal}, calorimetric enthalpy of unfolding; ΔH^{vH}, enthalpy of unfolding as calculated from the van't Hoff equation; T_m, melting temperature; C_{mid}, midpoint of transition; CD, circular dichroism.

[2] When referring to domains which are covalently attached, we use the terminology "A domain, B domain, C domain, BA domain, etc". When referring to the domains which have been subcloned and expressed separately, we use the nomenclature IIA^{mtl} for domain A of the mannitol-specific enzyme II, IIB^{mtl} for domain B of the mannitol-specific enzyme II, and $IIBA^{mtl}$ for domain BA of the mannitol-specific enzyme II. P_2-$IIBA^{mtl}$ refers to the doubly phosphorylated protein carrying one phosphoryl group on each domain.

0006-2960/96/0435-2759$12.00/0

domain. In principle, there are two possible observations that can be made when unfolding a multidomain protein: one can observe a single transition during which all domains unfold cooperatively, or one can observe multiple transitions, indicating that one or more relatively stable intermediates exist on the unfolding pathway. Examples of the former are lysozyme (Khechinashvili et al., 1973; Privalov & Khechinashvili, 1974), phosphoglycerate kinase (Hu & Sturtevant, 1987), and ribonuclease A (Brandts et al., 1989). Multiple transitions were observed in diphtheria toxin (Ramsay & Freire, 1990), pepsin and pepsinogen (Privalov et al., 1981), and human apotransferrin (Lin et al., 1994). The heat denaturation of yeast hexokinase exhibits both types of behavior depending on the presence or absence of the substrate glucose (Takahashi et al., 1981). The interpretation given to these observations is that multiple transitions indicate the absence of strong interdomain interactions whereas single transitions are an indication that the domains are strongly interacting. Using this model, one can thus obtain information on the extent of interaction between the domains in a multidomain protein.

In this study, information on the energetics of IIBA^{mtl} was obtained by unfolding studies using either GuHCl or heat as the denaturant, and the interaction between the two domains was quantitated by comparing the data to those obtained on the individual domains, IIA^{mtl} and IIB^{mtl}. The method was applied to the proteins in the unphosphorylated and phosphorylated states, enabling us to assess the interdomain interactions in IIBA^{mtl} as a function of the phosphorylation state of the enzyme.

MATERIALS AND METHODS

Protein Purification. IIBA^{mtl} was purified as described by van Weeghel et al. (1991b). IIA^{mtl} was purified as described by van Dijk et al. (1992a). IIB^{mtl} was purified as described by Robillard et al. (1993). Protein concentrations were determined spectrophotometrically using the absorbance of the tyrosine residues in the proteins. Extinction coefficients were determined by quantitative amino acid analysis of four solutions of each protein with known absorbance spectra. Values are $\epsilon = 6850\ M^{-1}\ cm^{-1}$ at 277 nm for IIA^{mtl}, $\epsilon = 3600\ M^{-1}\ cm^{-1}$ at 280 nm for IIB^{mtl}, and $\epsilon = 11\,000\ M^{-1}\ cm^{-1}$ at 278 nm for IIBA^{mtl}.

GuHCl-Induced Unfolding Studies. GuHCl-induced unfolding was studied by fluorescence and far-UV circular dichroism spectroscopy. All measurements were performed in 10 mM Hepes, pH 7.6, at a protein concentration of 4 μM. In each case, 2 mM mercaptoethanol was added to keep the active site cysteine of the B domain reduced. Proteins were incubated in GuHCl-containing solutions for at least 1 h at room temperature prior to measurements, except in the case of P-IIB^{mtl}. Incubation for longer periods up to 16 h did not change the results. In the case of P-IIB^{mtl}, equilibration was very rapid so that samples could be measured immediately after dilution in GuHCl-containing solutions. This approach reduced the risk of hydrolysis of the phosphoester bond during equilibration of the sample. All measurements were performed at 25 °C. The reversibility of the transitions was checked by diluting solutions of fully unfolded protein to a protein concentration of 4 μM and GuHCl concentrations well below the midpoint of transition. The signal of these solutions after equilibration was then compared to the signal of 4 μM protein solutions that had not been unfolded by GuHCl.

Protein Phosphorylation. Phosphorylated enzymes were obtained by adding 5 mM PEP, 5 mM $MgCl_2$, and catalytic amounts of EI, HPr, and IIA^{mtl} (in the case of IIB^{mtl} only) to the protein solution under study prior to dilution in GuHCl-containing solutions. Protein concentrations before dilution to 4 μM of the protein under study were 100 μM IIA^{mtl}, 5 μM HPr, and 0.5 μM EI in the case of P-IIA^{mtl}; 49 μM IIBA^{mtl}, 3 μM HPr, and 0.5 μM EI in the case of P_2-IIBA^{mtl}; and 96 μM IIB^{mtl}, 3 μM IIA^{mtl}, 6 μM HPr, and 0.5 μM EI in the case of P-IIB^{mtl}.

Spectroscopic Measurements. All fluorescence measurements were performed on an Aminco SPF 500 spectrofluorometer using 10 mm path length cells and 4 nm bandwidths for excitation and emission. Fluorescence emission spectra were recorded from 290 to 450 nm with the excitation wavelength at 277 nm. Fluorescence excitation spectra were recorded from 240 to 300 nm and monitored at 312 nm. Spectra were corrected for solvent emission and instrument response. Far-UV circular dichroism spectra were recorded from 260 to 195 nm on an Aviv 62A DS circular dichroism spectrometer in a 1 mm path-length cell and were corrected for absorption of the solvent. GuHCl titrations were monitored at 222 nm only, using one sample for every point of the titration and a 2 mm path-length cell. A point was obtained by monitoring the signal for 200 s and averaging.

Analysis of GuHCl-Induced Denaturation Curves. GuHCl-induced denaturation curves were converted to fractional changes by drawing linear base lines through the points in the pre- and posttransitional regions by least-squares analysis and extrapolating these into the transitional region. Where appropriate, the fractional change vs GuHCl concentration curves were analyzed using the linear extrapolation method (Pace, 1986; Santoro & Bolen, 1992). With this method, the free energy of unfolding, ΔG, is calculated as a function of the denaturant concentration by assuming a two-state mechanism and using the equation:

$$\Delta G = -RT \ln K_u = -RT \ln[(y_f - y_{obs})/(y_f - y_u)] \quad (1)$$

where y_f and y_u are values characteristic of the folded and unfolded proteins, respectively, and y_{obs} is the measured value at a stated denaturant concentration. ΔG can then be fit to the equation:

$$\Delta G = \Delta G(H_2O) - m[\text{GuHCl}] \quad (2)$$

where $\Delta G(H_2O)$ is the free energy in the absence of denaturant and m reflects the dependence of ΔG on the GuHCl concentration. Alternatively, by expressing f_u, the fractional change (equivalent to the fraction unfolded in the case of a two-state transition), as a function of the equilibrium constant

$$f_u = K_u/(K_u + 1) \quad (3)$$

and combining eqs 1, 2, and 3, a direct fit of the model to the fractional change can be obtained. The latter method is the one applied throughout this study.

Differential Scanning Calorimetry. Differential scanning calorimetry was performed on a MCS differential scanning calorimeter from Microcal with buffer in the reference cell. All scans were performed in 50 mM Hepes, pH 7.6, 10 mM

mercaptoethanol with a scan rate of 60 °C/h unless stated otherwise. All protein samples were extensively dialyzed with at least one change of buffer prior to measurements. Protein concentrations were around 90 μM for IIA^{mtl} and IIBA^{mtl} and around 180 μM for IIB^{mtl}. Scans were recorded from 5 to 85 °C or to higher temperatures. Rescans were performed to check for reversibility of the transition. To prevent the oxidation of mercaptoethanol by oxygen from the air during the calorimetric scan, all solutions were carefully degassed by stirring under vacuum for 15 min. This did not completely remove all oxygen so the remainder was left to react with the mercaptoethanol under nitrogen in the calorimeter at 35 °C for 30 min. Samples were subsequently cooled to the desired starting temperature, and a scan was recorded. The amount of reductant left in the solution after this procedure was above 80% of the original content as checked by reaction with 5,5′-dithiobis(2-nitrobenzoic acid) [see, e.g., Riddles et al. (1983) and references cited therein]. A buffer base line was subtracted, and the data were normalized to concentration and subsequently analyzed using the software package ORIGIN from Microcal.

RESULTS

Unfolding of IIA^{mtl}, IIB^{mtl}, and IIBA^{mtl}. The GuHCl-induced unfolding of IIA^{mtl}, IIB^{mtl}, and IIBA^{mtl} was studied using two spectroscopic probes, tyrosine fluorescence and circular dichroism. The results presented in Figure 1 for IIA^{mtl} and IIB^{mtl} (panels A and B, respectively) show one transition centered around 1.20 and 0.95 M GuHCl, respectively. It is immediately clear from the slope of the curves in the transitional region that the unfolding of IIA^{mtl} is more cooperative than the unfolding of IIB^{mtl}. Both transitions could be fitted well using the linear extrapolation method of Pace (1986) as shown by the good agreement of the dotted lines with the data. The $\Delta G(H_2O)$ values obtained from this are 27.6 kJ/mol and 12.3 kJ/mol for IIA^{mtl} and IIB^{mtl}, respectively; the values for *m* are 22.8 kJ/(mol·M) and 13.1 kJ/(mol·M). The latter two values reflect the higher cooperativity of the IIA^{mtl} transition. The unfolding of IIBA^{mtl} (panel C), as monitored by the change in ellipticity at 222 nm, clearly exhibits two stages: the fraction unfolded increases gradually from 0 to 0.2 between 0 and 0.8 M GuHCl and then rises rapidly from 0.2 to 1 between 0.8 and 1.5 M GuHCl. From comparison with the unfolding profiles of the individual domains, it is clear that the gradual change at lower GuHCl concentrations corresponds to the unfolding of the B domain and the cooperative transition at higher GuHCl concentrations corresponds to the unfolding of the A domain. Data obtained from fluorescence and CD show a good correspondence in the case of IIA^{mtl} and IIB^{mtl}, but not for IIBA^{mtl}. This discrepancy is caused by the peculiar properties of the one tyrosine residue in IIB^{mtl}.

Figure 2 shows fluorescence excitation and emission spectra and CD spectra of IIB^{mtl} as a function of pH. The excitation and emission maxima of tyrosine residues in proteins are typically 278 and 305 nm, respectively. These values are observed below pH 4 for the one tyrosine residue in IIB^{mtl}, but at pH 6.1, 6., and 7.9, a band of lower intensity with an excitation maximum around 282 nm and an emission maximum around 320 nm is visible. At pH values between 4 and 6, intermediate values are found for both the intensity and λ_{max} in the fluorescence spectra. This behavior is typical of a species that has at least partial tyrosinate character.

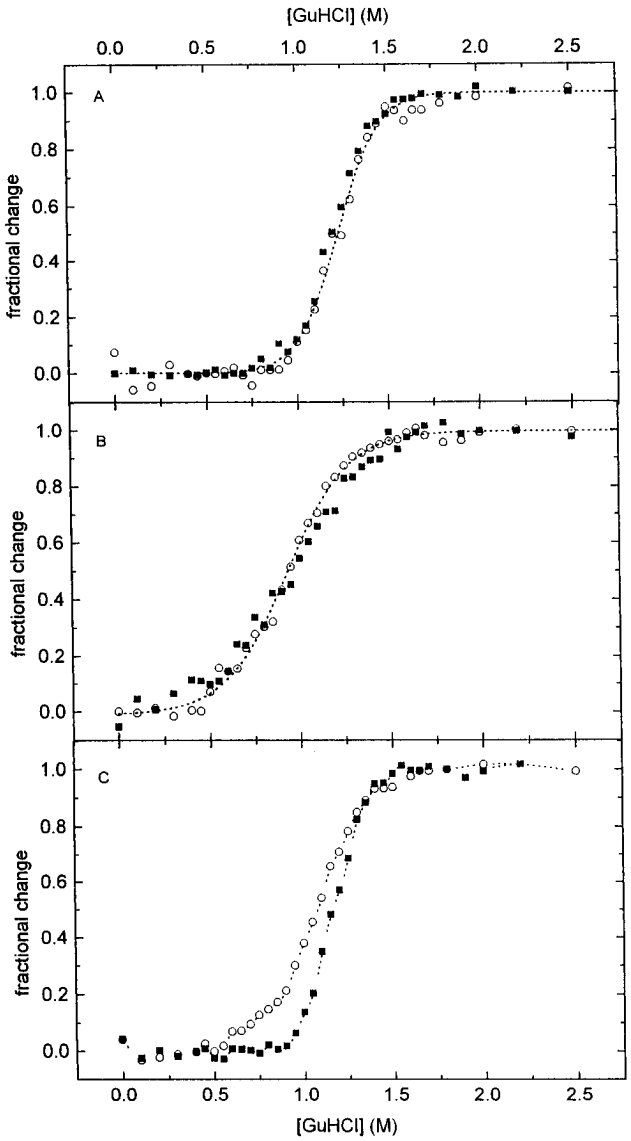

FIGURE 1: GuHCl-induced unfolding of IIA^{mtl} (A), IIB^{mtl} (B), and IIBA^{mtl} (C) in 10 mM Hepes, pH 7.6, 2 mM β-mercaptoethanol at 25 °C. Protein concentrations were 4 μM in each case. The dotted lines through the data are least-squares fits to the LEM equation in (A) and (B) and linear connections of the points in (C). (○) Circular dichroism at 222 nm; (■) fluorescence at 305 nm.

Similar observations have been made for a number of other proteins [see, e.g., Pundak and Roche (1984) and references cited therein] although the emission bands were usually at longer wavelengths (330−350 nm). One question to answer is whether this tyrosinate is present in the ground state or is formed in the excited state by excited state proton transfer to an acceptor in the direct vicinity. Since the pK_a of a tyrosine residue is normally around 10 (Glazer, 1976), a strong pH dependence of both the emission and excitation spectra is expected for a ground state tyrosinate. This is not observed for IIB^{mtl} in the pH interval 6−8. Increasing tyrosine character is observed with decreasing pH, below pH 6, but the circular dichroism spectra (panel C) show that the protein is also unfolding below pH 6. Since the excitation and emission spectra are essentially independent of pH down to pH 6 and the protein begins to unfold below pH 6, we can only conclude that either (i) tyrosinate is present in the ground state but its pK_a is below 6 or (ii) tyrosinate is only formed in the excited state.

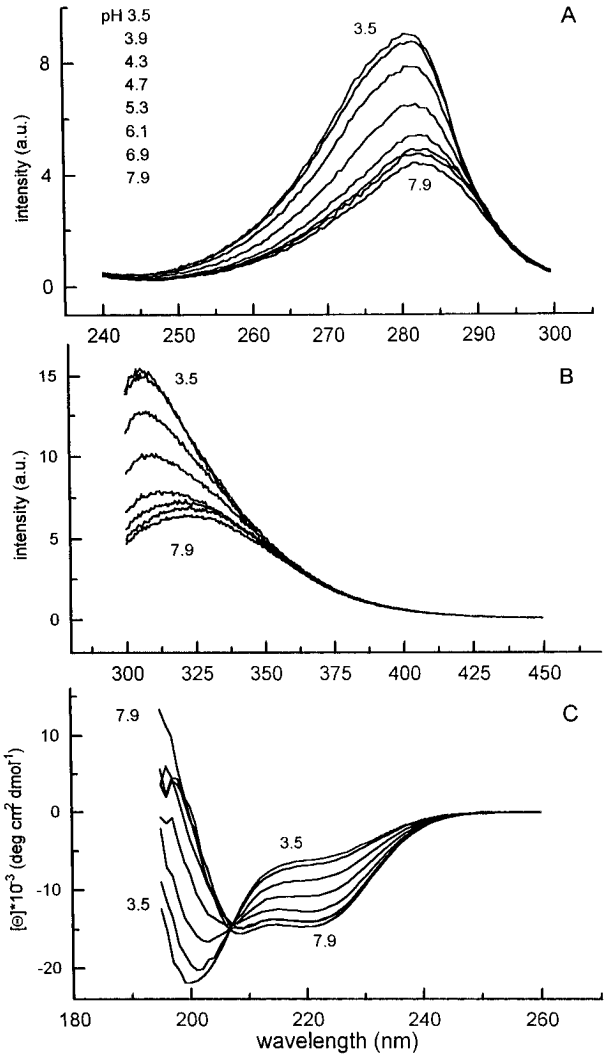

FIGURE 2: Fluorescence excitation, fluorescence emission, and circular dichroism spectra of IIB^{mtl} as a function of pH. Experimental conditions were 10 mM citrate, 1 mM gluthathione except for the sample at pH 7.9: 10 mM phosphate, 1 mM gluthathione. (A) Fluorescence excitation spectra, emission wavelength 312 nm. (B) Fluorescence emission spectra, excitation wavelength 277 nm. (C) Circular dichroism spectra.

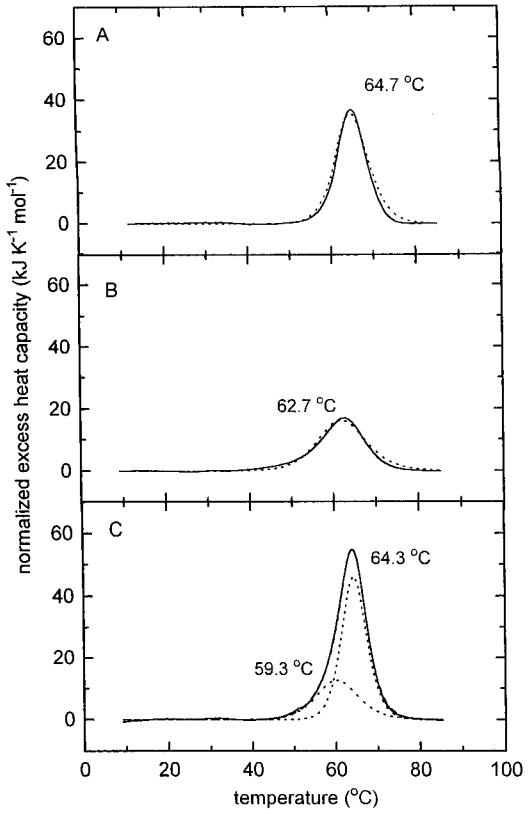

FIGURE 3: Excess heat capacity function versus temperature for 94 μM IIA^{mtl} (A), 198 μM IIB^{mtl} (B), and 86 μM IIBA^{mtl} (C). Experimental conditions were 50 mM Hepes, pH 7.6, 10 mM β-mercaptoethanol; the scanning rate was 60 °C/h. The experimental curves shown in the figure were obtained by (i) subtracting a buffer−buffer base line, (ii) normalization to concentration, and (iii) subtracting a base line based on how far the transition was from completion. Solid lines are the experimental curves; dotted lines are the theoretical fits to the data using a two-state model in the case of IIA^{mtl} and IIB^{mtl} and a non-two-state model in the case of IIBA^{mtl}.

The thermal denaturation of IIBA^{mtl} and its individual domains was studied by differential scanning calorimetry. Figure 3 shows typical examples of the excess heat capacity curves as a function of temperature for the three proteins. The two-state fits to the IIA^{mtl} and IIB^{mtl} transitions and the deconvolution analysis of the transition of IIBA^{mtl} are also shown. In each case, there is a good agreement between the observed data and the theoretical fits. The melting temperatures (defined here as the temperatures at which maximum heat absorption occurs) for IIA^{mtl} and IIB^{mtl} are 64.7 and 62.7 °C, respectively, and the corresponding. unfolding enthalpies are 377 and 260 kJ/mol, respectively. The transition of IIA^{mtl} is, again, the more cooperative of the two as evidenced by the 8 °C width at half-height for IIA^{mtl} compared to 11 °C for IIB^{mtl}. Reversibility of the transitions was judged by the reappearance of the heat absorption peak in rescans of the samples and was around 90% for IIA^{mtl} and around 60% for IIB^{mtl}. The latter value is rather low due to a slow aggregation process taking place in the unfolded state. To ensure that the sample was in equilibrium throughout the run, the scan-rate dependence of the observed transition was checked. No dependence from either the melting temperature or the enthalpy of unfolding was found in the interval ranging from 12 °C/h to 120 °C/h.

The thermal unfolding profile of IIBA^{mtl} exhibits one large peak with maximal heat absorption at 64.3 °C. The total enthalpy of unfolding of IIBA^{mtl} is 531 kJ/mol, which, surprisingly, is lower than the sum of the enthalpies of IIA^{mtl} and IIB^{mtl} (637 kJ/mol). Deconvolution analysis showed that the unfolding of IIBA^{mtl} could be best described by two overlapping transitions centered around 59.3 and 64.3 °C. The former transition is rather broad and corresponds to a calorimetric enthalpy of unfolding of 156 kJ/mol whereas the latter is sharper and more intense, corresponding to a calorimetric enthalpy of 378 kJ/mol. The $\Delta H^{cal}/\Delta H^{vH}$ ratios were 0.53 and 0.77, respectively; neither transition was of a two-state character. The reversibility of the IIBA^{mtl} scans was around 90%. All parameters obtained from the DSC studies are listed in Table 2.

Unfolding of the Phosphorylated Forms of IIA^{mtl}, IIB^{mtl}, and IIBA^{mtl}. The stabilities of the phosphorylated species of IIA^{mtl}, IIB^{mtl}, and IIBA^{mtl} were studied by GuHCl-induced unfolding only. Thermal unfolding of these species could not be monitored due to (i) the thermal inactivation of EI and (ii) the increase of the rate of hydrolysis of the phosphoester bond at elevated temperatures. The GuHCl-induced unfolding transition of P-IIA^{mtl} deviated clearly from

Table 1: Analysis of GuHCl-Induced Unfolding Curves Using the Linear Extrapolation Method[a]

protein	C_{mid} (M GuHCl)	m (kJ mol^{-1} M^{-1})	$\Delta G(H_2O)$ (kJ mol^{-1})
IIA^{mtl}	1.21	22.8 (1.3)	27.6 (1.6)
P-IIA^{mtl}	0.83	19.1 (2.0)	15.8 (1.7)
IIB^{mtl}	0.95	13.1 (0.6)	12.3 (0.6)
P-IIB^{mtl}	0.86	15.7 (1.4)	13.9 (1.2)
IIBA^{mtl}	1.07 (CD), 1.17 (flu)		
P-IIBA^{mtl}	0.89 (CD), 0.92 (flu)		

[a] Values in parentheses are the standard deviations obtained from the fit to the experimental data.

Table 2: Thermal Unfolding of IIA^{mtl}, IIB^{mtl}, and IIBA^{mtl} [a]

protein	scan rate (°C h^{-1})	T_m (°C)	ΔH^{cal} (kJ mol^{-1})	ΔH^{vH} (kJ mol^{-1})	$\Delta H^{cal}/\Delta H^{vH}$
IIA^{mtl} [b]	60	66.7 (0.05)	341 (4)	378 (3)	0.90 (0.01)
	60	64.7 (0.3)	340 (8)	377 (3)	0.90 (0.02)
IIB^{mtl}	60	62.7 (0.04)	268 (4)	260 (2)	1.03 (0.02)
	12	63.7	311	311	1.00
	30	63.6	257	289	0.89
	90	64.0	301	313	0.96
	120	64.7	314	314	1.00
IIBA^{mtl}	60	59.3	156 (12)	298 (11)	0.53 (0.1)
	60	64.3	378 (15)	490 (4)	0.77 (0.04)

[a] Experimental conditions were 50 mM Hepes, pH 7.6, 10 mM β-mercaptoethanol. Values in parentheses are standard deviations derived from averaging at least three experiments but indicate only the reproducibility of the scans. The actual errors are estimated to be 0.5 °C for T_m and 10% for ΔH^{cal}. The measurements reported in the first row were done in the absence of mercaptoethanol. From the good correspondence between the data in the first two rows, it is clear that the procedure used to remove oxygen from the solutions does not influence the results. [b] Experimental conditions: no mercaptoethanol present.

the unfolding transition of the unphosphorylated IIA^{mtl} (Figure 4A). The midpoint of transition is shifted to 0.8 M GuHCl, i.e., 0.4 M GuHCl lower than the midpoint of IIA^{mtl}. The $\Delta G(H_2O)$ as calculated from the LEM is also lower: 14.6 kJ/mol vs 27.6 kJ/mol. In addition, the transition is also less cooperative: the value for m is lowered by 15% from 22.8 to 19.7 kJ/(mol·M) GuHCl. For the phosphorylated IIB^{mtl}, the situation is different (Figure 4B): the midpoint of transition is shifted only marginally to 0.86 M, and the $\Delta G(H_2O)$ is essentially the same (13.9 kJ/mol for P-IIB^{mtl} compared to 12.3 kJ/mol for IIB^{mtl}). These data indicate that phosphorylation has a much larger impact on the stability of IIA^{mtl} than on the stability of IIB^{mtl}.

Since no difference could be observed between the GuHCl-induced unfolding curves of IIB^{mtl} and P-IIB^{mtl}, it was necessary to establish that the phosphoester bond of P-IIB^{mtl} had not been hydrolyzed during the process of unfolding. To this end, concentrated solutions of IIB^{mtl} and P-IIB^{mtl} were unfolded in 1.5 M GuHCl, left in the unfolded state for approximately 5 min (the time required to obtain a point for the GuHCl titration), and then diluted in buffer to a concentration of 0.3 M GuHCl. The diluted samples as well as IIB^{mtl} and P-IIB^{mtl} samples that had not been exposed to GuHCl were subjected to nondenaturing polyacrylamide gel electrophoresis in order to distinguish between the two species on the basis of their charge difference. Figure 5A shows that P-HPr migrated much faster than HPr (lane 2 *versus* lane 1). The same tendency is seen for IIA^{mtl} (lane 5 *versus* lane 4) and IIB^{mtl} (lane 8 *versus* lane 7), but the shifts are less dramatic. Figure 5B shows that the same phosphorylation-induced shift is present with P-IIB^{mtl} after GuHCl denaturation and refolding as before denaturation.

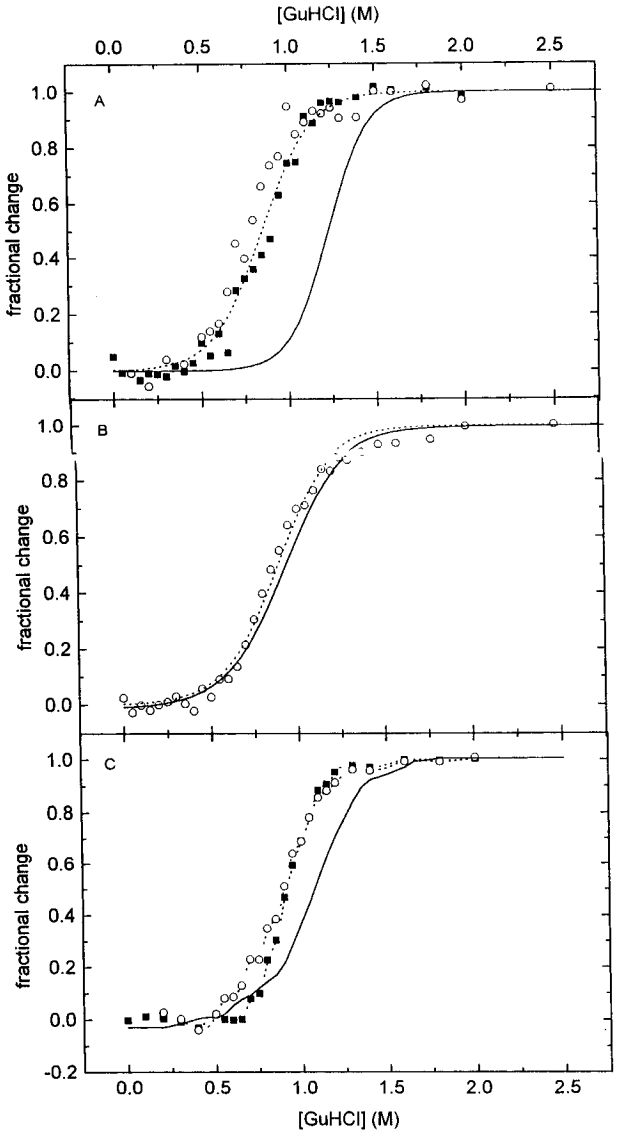

FIGURE 4: GuHCl-induced unfolding of P-IIA^{mtl} (A), P-IIB^{mtl} (B), and P-IIBA^{mtl} (C) in 10 mM Hepes, pH 7.6, 2 mM β-mercaptoethanol at 25 °C. Protein concentrations were 4 μM in each case. The dotted lines through the data are least-squares fits to the LEM equation in (A) and (B) and linear connections of the points in (C). Solid lines indicate the unfolding transitions of the corresponding unphosphorylated proteins. (○) Circular dichroism at 222 nm; (■) fluorescence at 305 nm.

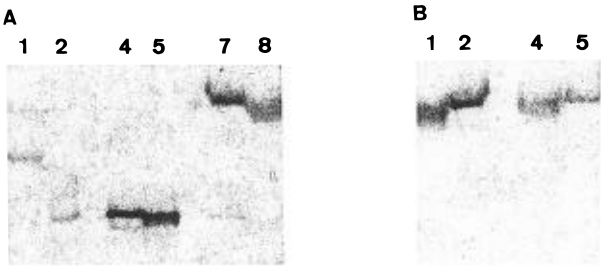

FIGURE 5: Nondenaturing polyacrylamide gels of PTS components. (A) Lane 1, HPr; lane 2, P-HPr; lane 4, IIA^{mtl}; lane 5, P-IIA^{mtl}; lane 7, IIB^{mtl}; lane 8, P-IIB^{mtl}. (B) Lanes 1 and 2, P-IIB^{mtl} and IIB^{mtl} prior to treatment with GuHCl; lanes 3 and 4, P-IIB^{mtl} and IIB^{mtl} after unfolding in 1.5 M GuHCl and refolding (see Materials and Methods for details).

From these patterns, it is clear that P-IIB^{mtl} is not hydrolyzed during unfolding in the time span of the experiment.

The GuHCl-induced unfolding profiles of phosphorylated IIBA^{mtl} monitored by fluorescence and circular dichroism are shown in Figure 4C. As in the case of IIA^{mtl}, the midpoint of transition is shifted toward lower GuHCl concentrations upon phosphorylation. This phenomenon is independent of the technique that is used to monitor the transition, although the magnitude of the effect is larger in the case of tyrosine fluorescence than in the case of CD (0.25 and 0.18 M GuHCl, respectively). This reflects the fact that the stability of the A domain, the only domain observed using tyrosine fluorescence, is more affected than the stability of the B domain upon phosphorylation of IIBA^{mtl}. The unfolding profiles of P_2-IIBA^{mtl} monitored by tyrosine fluorescence and circular dichroism do not match, in much the same way as in the case of unphosphorylated IIBA^{mtl}, though the difference is smaller than in the unphosphorylated case. The latter is not unexpected since the midpoints of transition of P-IIA^{mtl} and P-IIB^{mtl} are very close. The discrepancy between the fluorescence and CD data sets for P_2-IIBA^{mtl} indicates that the unfolding of P_2-IIBA^{mtl} is not a two-state process. What is observed are two independent transitions that are very close together, not one cooperative transition from the folded to the unfolded state. A much better way to discriminate between the two possibilities would be comparing the calorimetric and the van't Hoff enthalpies obtained from DSC experiments. This, however, is not possible due to hydrolysis of the P-protein and inactivation of EI mentioned above.

In the case of the unphosphorylated enzymes, we found a destabilization of IIBA^{mtl} with respect to the free IIA^{mtl} and IIB^{mtl}. Unfortunately, the unfolding transitions of the domains in P_2-IIBA^{mtl} were barely separated, and, as a result of the overlap, we were unable to obtain a value for the free energy of the interaction. The mere existence of two unfolding transitions in P_2-IIBA^{mtl} as in IIBA^{mtl} does seems to suggest, however, that there is not much difference between the interactions of the A and B domains in the unphosphorylated and the phosphorylated state.

DISCUSSION

GuHCl-Induced Unfolding. The GuHCl-induced unfolding curves measured both by tyrosine fluorescence and by circular dichroism of IIA^{mtl} and IIB^{mtl} show good correspondence with the theoretical curves calculated by the LEM. Since this approach assumes a two-state character of the transition, the correspondence is good evidence that, indeed, both proteins exhibit such behavior. This is not unexpected; many small globular proteins have been shown to change their conformation cooperatively from the native to the fully unfolded form without significantly populating an intermediate state during the process. In contrast to IIA^{mtl} and IIB^{mtl}, the binary combination of the two domains, IIBA^{mtl}, does not show typical two-state behavior. This is most clearly seen in the CD data. The initial gradual change, indicating a transition that is not very cooperative, corresponds to the unfolding of the B domain, while the subsequent steep increase in the fraction unfolded corresponds to the unfolding of the A domain.

Comparison of the fluorescence spectra and the CD spectra of IIB^{mtl} clearly indicates that the change from a tyrosinate to a tyrosine and the unfolding of the protein occur concomitantly. The isosbestic point at 307 nm in the circular dichroism spectra confirms that the acid-induced unfolding of IIB^{mtl} is a two-state process. The discrepancy between the fluorescence and CD data for unfolding of IIBA^{mtl} is caused by the fluorescent properties of the tyrosine residue in the B domain. The excited state tyrosinate is strongly quenched so that its intensity is much lower than that of the four tyrosines in the A domain. Upon unfolding of the B domain, the change of tyrosinate to tyrosine is accompanied by an increase in intensity and a shift of the emission maximum to lower wavelengths. The unfolding of the A domain results in a decrease in intensity at the same wavelength where the largest intensity increase is found for the B domain. Since both transitions are very close and the number of tyrosines in the A domain is 4 times larger than in the B domain, the changes in fluorescence as a function of the GuHCl concentration are totally dominated by the changes arising from the unfolding of the A domain. CD provides a less biased picture of the unfolding since both the A and B domains contain a fair amount of α helix and the ellipticity of IIBA^{mtl} at 222 nm reflects changes in both domains. The fact that the transition observed by fluorescence measurements begins at higher GuHCl concentrations than the transition monitored by CD indicates that the A domain is the most stable of the two domains in IIBA^{mtl}.

Differential Scanning Calorimetry. Interpretation of scanning calorimetry data is based on models that apply to equilibrium thermodynamics. It is, therefore, important to establish whether or not equilibrium is maintained during the calorimetric runs. In general, this is done by checking the reversibility of the transition, that is, the reappearance of the heat absorption peak in a rescan of the same sample. The rescans that were performed on the DSC samples in this study indicated that reversibility was greater than 90% for IIA^{mtl} and IIBA^{mtl}. It was lower for IIB^{mtl} which showed a reduction in total heat absorption of about 40% in rescans. This was caused by a slow aggregation process that occurred after unfolding. Sturtevant (Sturtevant, 1987; Manly et al., 1985; Edge et al., 1985, 1988; Hu & Sturtevant, 1987) has shown that equilibrium models can be applied to scanning calorimetric data that show no reappearance of heat absorption peaks in rescans provided that the reaction causing the irreversibility takes place after unfolding has been completed. The scan rate independence of the calorimetric data for IIB^{mtl} shows that equilibrium is indeed maintained throughout the unfolding process. It is, therefore, justified to use equilibrium methods to interpret all scanning calorimetric data in this study. The heat-induced unfolding of IIBA^{mtl}, IIA^{mtl}, and IIB^{mtl} is, in general, in good agreement with the data from the GuHCl-induced unfolding. In both cases, IIB^{mtl} is less stable and unfolds less cooperatively than IIA^{mtl}, both in IIBA^{mtl} and as a free protein. The two-state character of the unfolding of IIA^{mtl} and IIB^{mtl} is also clear from the $\Delta H^{cal}/\Delta H^{vH}$ ratios close to 1. The value for IIA^{mtl} shows the largest deviation from unity but this is probably caused by some aggregation in the native state of the protein, a feature that has been observed for this particular protein regularly in our laboratory.

Influence of Domain Interactions and Phosphorylation. When deconvoluting the heat absorption peak of IIBA^{mtl}, it was found that a good fit could only be obtained assuming two transitions and a non-two-state-model for both transi-

tions. Comparing the results from this analysis with those obtained on the free hydrophilic domains, and bearing in mind that the B domain was also less stable than the A domain when unfolding was studied using GuHCl as the denaturant, it seems justified to assign the lower temperature transition to the B domain and the higher temperature transition to the A domain. From the fact that the total enthalpy of unfolding of IIBA^{mtl} is lower than the sum of the enthalpies from the transitions of IIA^{mtl} and IIB^{mtl}, it is obvious that there is some sort of interaction between the domains, though not a stabilizing one. This interaction could also cause the deviation from a two-state unfolding mechanism that is observed for both transitions. The main destabilizing effect is on the B domain which is lower in melting temperature by 3 °C and lower in unfolding enthalpy by 100 kJ/mol when present in IIBA^{mtl}. The enthalpies of unfolding of IIA^{mtl} and IIB^{mtl} themselves are rather low when they are compared to the enthalpies of unfolding of other globular proteins on a per residue basis (Makhatadze & Privalov, 1994). In a recent paper, Wintrode et al. (1995) have reported a similar low value for the enthalpy of unfolding of Barstar. Two components contribute to the enthalpy of unfolding: the enthalpy of hydration and the enthalpy of internal interactions. The authors showed that the enthalpy of hydration per amino acid residue was similar to that of other proteins but that the enthalpy of internal interactions was significantly lower. The authors suggest that the low value results from a loosely packed protein interior which could facilitate the interaction of Barstar with Barnase since it would be possible to rearrange the structure of Barstar without the disruption of energetically favorable interactions. IIB^{mtl} has the same enthalpy of unfolding at its T_M as Barstar at that temperature while the enthalpy of unfolding of the B domain in IIBA^{mtl} is considerably lower; it is one of the lowest reported. Since we do not yet have high-resolution structures of these proteins, the enthalpies of unfolding cannot be separated into contributions from hydration and internal interactions as was done for Barstar. A good degree of conformational flexibility, however, is to be expected in order to achieve rapid rates of phosphoryl group transfer. For such transfers, IIA^{mtl} must interact optimally withHPr and IIB^{mtl} while IIB^{mtl} must interact with IIA^{mtl} and IIC^{mtl}. Whether the decrease of the enthalpy of unfolding of the B domain in IIBA^{mtl} is due to a loosening of the internal interactions, changes in hydration, or a substantially different conformation awaits high-resolution structures on the isolated and fused proteins.

In a number of other cases, interactions between domains resulting in a destabilization of the protein with respect to the individual free domains in solution were observed. Potekhin and Privalov (1982) showed that adjacent cooperative blocks in tropomyosin were mutually destabilized and suggested that this was related to the relief of stress in the coiled-coil type of structure that is normally formed by this protein. In the PTS enzyme I from *S. typhimurium*, it was found that the melting temperature of the free 30 kDa N-terminal protease fragment was higher than the melting temperature of the corresponding domain in the intact enzyme (LiCalsi et al., 1991), but no explanation for this behavior was given. Markovic-Housley et al. (1994) observed a destabilization of the B domain in IIBA^{man} relative to that of the isolated protein. This was reported by a 4 °C decrease in T_m comparable to that observed above for the mannitol system. Unfortunately, IIB^{man} began to precipitate during the melting transition, preventing a measurement of the enthalpy of unfolding for comparison with that of the B domain in IIBA^{man}. The T_m shifts for the B domain in the fused *versus* isolated protein in the mannitol and mannose systems are so similar that we can assume that IIB^{man} also experiences a decrease in unfolding enthalpy in the fused state. Since no stabilizing B/A domain interaction was observed, the authors suggested that the need for a high local concentration was the reason for the covalent attachment of the domains. This explanation is applicable to IIBA^{mtl} as well. One cannot rule out, however, the possibility that the low enthalpies of unfolding are a result of the artificial experimental system. In the mannitol-specific system, the B domain is covalently linked to the C domain while in the mannose-specific system the IIBA^{man} and IICD^{man} subunits are tightly associated. In both cases, the destabilizing interactions between the A and B domains might be more than compensated by interactions between the B domain and the membrane-bound domains. Investigations are currently in progress to examine this possibility.

The transport of mannitol can only take place if the hydrophilic domains of EII^{mtl} cycle through a phosphorylation/dephosphorylation sequence. Therefore, the interdomain interactions of the phosphorylated proteins have to be investigated to correlate their behavior with the transport process. Phosphorylation of IIA^{mtl} and IIBA^{mtl}, but not IIB^{mtl}, leads to destabilization of the protein. At the present time, there are not sufficient structural details available on these proteins to explain these observations; however, the three-dimensional structures of IIA^{glc} from *E. coli* and *B. subtilis* are available (Pelton et al., 1991a,b; Fairbrother et al., 1992; Worthylake et al., 1991; Liao et al., 1991), and it is not unreasonable to assume that the structures of IIA^{glc} and IIA^{mtl} are similar in the vicinity of the active site since both proteins are phosphorylated by P-HPr. The active site histidine of IIA^{glc} is situated in a shallow depression and surrounded by a hydrophobic patch. This could have a structuring effect on water in the immediate vicinity of the active site. Since the phosphate group has a large tendency for hydration (Urry, 1993), water structure will be largely disrupted, thus destabilizing the protein. In contrast, the active site of IIB^{glc} and IIB^{mtl} from *E. coli* was found to be highly reactive and proposed to be on the surface of the protein (Golic Grdadolnik et al., 1994, AB et al., unpublished observations). The phosphoryl group attached to the cysteine would then be exposed to the solvent, having little effect on the structural stability of the protein. More detailed structural studies will be necessary in order to gain quantitative insight into the factors that govern the structural stability of IIA^{mtl}, IIB^{mtl}, and IIBA^{mtl} and how these factors change upon phosphorylation. These studies are in progress.

REFERENCES

Boer, H., Ten Hoeve-Duurkens, R. H., Lolkema, J. S., & Robillard, G. T. (1995) *Biochemistry 34*, 3239−3247.

Brandts, J. F., Hu, C. Q., Lin, L.-N., & Mas, M. T. (1989) *Biochemistry 28*, 8588−8596.

Edge, V., Allewell, N. M., & Sturtevant, J. M. (1985) *Biochemistry 24*, 5899−5906.

Edge, V., Allewell, N. M., & Sturtevant, J. M. (1988) *Biochemistry 27*, 8081−8087.

Glazer, A. N. (1976) in *The Proteins* (Neurath, H., & Hill, R. L., Eds.), 3rd ed., Vol. 2, pp 1−103, Academic Press, New York.

Golic Grdadolik, S., Eberstadt, M., Gemmecker, G., Kessler, H., Buhr, A., & Erni, B. (1994) *Eur. J. Biochem. 219*, 945−952.
Hu, C. Q., & Sturtevant, J. M. (1987) *Biochemistry 26*, 178−182.
Khechinashvili, N. N., Privalov, P. L., & Tiktopulo, E. I. (1973) *FEBS Lett. 30*, 57−60.
Kroon, G. J. A., Grötzinger, J., Dijkstra, K., Scheek, R. M., & Robillard, G. T. (1993) *Protein Sci. 2*, 1331−1341.
Liao, D.-I., Kapadia, G., Reddy, P., Saier, M. H., Reizer, J., & Herzberg, O. (1991) *Biochemistry 30*, 9583−9594.
LiCalsi, C. L., Crocenzi, T. S., Freire, E., & Roseman, S. (1991) *J. Biol. Chem. 266*, 19519−19527.
Lin, L.-N., Mason, A. B., Woodworth, R. C., & Brandts, J. F. (1994) *Biochemistry 33*, 1881−1888.
Lolkema, J. S., & Robillard, G. T. (1992) *New Compr. Biochem. 21*, 135−168.
Makhatadze, G. I., & Privalov, P. L. (1995) *Biophys. Chem. 51*, 291−309.
Manly, S. P., Matthews, K. S., & Sturtevant, J. M. (1985) *Biochemistry 24*, 3842−3846.
Markovic-Housley, Z., Cooper, A., Lustig, A., Flükiger, K., Stolz, B., & Erni, B. (1994) *Biochemistry 33*, 10977−10984,
Pace, C. N. (1986) *Methods Enzymol. 131*, 266−280,
Pas, H. H., & Robillard, G. T. (1988) *Biochemistry 27*, 5835−5839,
Pas, H. H., Ten Hoeve-Duurkens, R. H., & Robillard, G. T. (1988) *Biochemistry 27*, 5520−5525,
Pas, H. H., Meyer, G., Kruizinga, W. H., Tamminga, K. S., Van Weeghel, R. P., & Robillard, G. T. (1991) *J. Mol. Biol. 266*, 6690−6692,
Pelton, J. G., Torchia, D. A., Meadow, N. D., Wong, C.-Y., & Roseman, S. (1991a) *Proc. Natl. Acad. Sci. U.S.A. 88*, 3479−3483.
Pelton, J. G., Torchia, D. A., Meadow, N. D., Wong, C.-Y., & Roseman, S. (1991b) *Biochemistry 30*, 10043−10057.
Postma, P. W., Lengeler, J. W., & Jacobson, G. R. (1993) *Microbiol. Rev. 57*, 543−574.
Potekhin, S. A., & Privalov, P. L. (1982) *J. Mol. Biol. 159*, 519−535.
Privalov, P. L., & Khechinashvili, N. N. (1974) *J. Mol. Biol. 86*, 665−684.
Privalov, P. L., Mateo, P. L., Khechinashvili, N. N., Stepanov, V. M., & Revina, L. P. (1981) *J. Mol. Biol. 152*, 445−464.
Pundak, S., & Roche, R. S. (1984) *Biochemistry 23*, 1549−1555.
Ramsay, G., & Freire, E. (1990) *Biochemistry 29*, 8677−8683.
Riddles, P. W., Blakeley, R. L., & Zerner, B. (1983) *Methods Enzymol. 91*, 49−60.
Robillard, G. T., Boer, H., van Weeghel, R. P., Wolters, G., & Dijkstra, A. (1993) *Biochemistry 32*, 9553−9562.
Santoro, M. M., & Bolen, D. W. (1992) *Biochemistry 31*, 4901−4907.
Sturtevant, J. M. (1987) *Annu. Rev. Phys. Chem. 38*, 463−488.
Takahashi, K., Casey, J. L., & Sturtevant, J. M. (1981) *Biochemistry 20*, 4693−4697.
Urry, D. W. (1993) *Angew. Chem., Int. Ed. Engl. 32*, 819−841.
Van Dijk, A. A., Scheek, R. M., Dijkstra, K., Wolters, G. K., & Robillard, G. T. (1992a) *Biochemistry 31*, 9063−9072.
Van Weeghel, R. P., Meyer, G. H., Keck, W., & Robillard, G. T. (1991a) *Biochemistry 30*, 1774−1779.
Van Weeghel, R. P., Meyer, G. H., Pas, H. H., Keck, W., & Robillard, G. T. (1991b) *Biochemistry 30*, 9478−9485.
Wintrode, P. L., Griko. Y. V., & Privalov, P. L. (1995) *Protein Sci. 4*, 1528−1534.
Worthylake, D., Meadow, N. D., Roseman, S., Liao, D. I., Herzberg, O., & Remington, S. J. (1991) *Proc. Natl. Acad. Sci. U.S.A. 88*, 10382−10386.

BI952567B